Adsorption (2012) 18:423–430
DOI 10.1007/s10450-012-9428-9

Selective adsorption of CO_2 on amino-functionalized silica spheres with centrosymmetric radial mesopores and high amino loading

Shiyou Hao · Jing Zhang · Yijun Zhong · Weidong Zhu

Received: 18 May 2012 / Accepted: 20 September 2012 / Published online: 2 October 2012

Abstract Amino-functionalized silica spheres with centrosymmetric radial mesopores and high amino loading were synthesized using the anionic surfactant N-lauroylsarcosine sodium (Sar-Na) as template and 3-aminopropyltrimethoxysilane (APTMS) as co-structure directing agent (CSDA) by an orthogonal experiment optimization. The synthesized amino-functionalized mesoporous silica (AFMS) was used as adsorbent to the selective adsorption of CO_2. The effects of water vapor in the adsorptive stream on the adsorption properties of CO_2 were investigated in detail. The results show that the synthesized adsorbent possesses a high adsorption selectivity for CO_2 over CH_4 and N_2 due to the specific interactions between CO_2 and amino groups. The presence of water vapor in the adsorptive stream can dramatically enhance the adsorbed amount of CO_2 because of the partial formation of bicarbonate in the presence of moisture. Furthermore, the adsorbent shows a good stability, confirmed by adsorption-regeneration cycles. Based on these excellent properties, the application of the developed AFMS adsorbent in the selective adsorption of CO_2 is anticipated.

Keywords Amino-functionalized mesoporous silica · CO_2 adsorption · Separation · Water vapor effect · Natural gas purification

S. Hao (✉) · J. Zhang · Y. Zhong · W. Zhu
Key Laboratory of the Ministry of Education for Advanced Catalysis Materials, Institute of Physical Chemistry, Zhejiang Normal University, 321004 Jinhua, P.R. of China
e-mail: sky54@zjnu.cn

W. Zhu (✉)
e-mail: weidongzhu@zjnu.cn

1 Introduction

Carbon dioxide (CO_2) has become an important global issue due to the gradual increase in the atmospheric concentration of CO_2 resulted from fossil fuel combustion and the link between an increase in the concentration of CO_2 in the atmosphere and global climate changes. Therefore, it is necessary to reduce CO_2 concentration significantly from the current level (Song 2006). Up to now, various technologies, such as amine solutions for absorption, membrane separation, and adsorption-based separation, have been employed to stabilize the CO_2 concentration in the atmosphere by controlling the emission of CO_2 from various sources (Na et al. 2002; Sandru et al. 2009; Veawab et al. 1999). However, a large amount of energy required for the regeneration of the used amine solutions, equipment corrosion, and degradation of amine solutions in the presence of oxygen are often associated with amine solutions for CO_2 absorption (Lawal et al. 2005; Veawab et al. 2001). The membrane-separation technology is always suffering from scale-up difficulty and high cost (Bhide et al. 1998). Adsorption, in fact, has become the state of the art technology for the separation and recovery of CO_2 (Zelenak et al. 2008). Although the conventional activated carbons and zeolites possess relatively high CO_2 adsorption capacities at room temperature, the adsorbed amounts of CO_2 on these adsorbents will decline rapidly with increasing temperature. Additionally, the adsorption selectivity for CO_2 on activated carbons and zeolites in the presence of water vapor will become very poor (Himeno et al. 2005). At high temperatures, hydrotalcites can adsorb CO_2 but their adsorption capacities towards CO_2 are, in general, low and basic metal oxides such as MgO and CaO have extremely large absorption capacities for CO_2 but the regeneration of these absorbents is performed at higher temperatures, resulting in severe energy penalties (Kim et al.

2005). Therefore, the development of efficient adsorbents is of utmost importance for CO_2 capture and separation.

Amino-functionalized mesoporous silicas could be ideal adsorbents for capturing or separating CO_2 due to the reversible formation of ammonium carbamates and/or carbonates during CO_2 adsorption, leading to a high selectivity for CO_2 over alkanes and N_2 (Belmabkhout et al. 2010; Hao et al. 2011). Generally, two synthesis methods, i.e., post-grafting and co-condensation, have been applied to the preparation of AFMS (Da'na and Sayari 2011; Du and He 2012). The post-grafting method, however, often gives rise to an inhomogeneous surface coverage due to organic moieties congregating near the entries of the mesopores and the exterior surface of the resulting AFMS (Richer and Mercier 1998). The co-condensation method may lead to situations where some of the functional groups are embedded in the silica network, and the co-condensation of organosilanes with terminal organic groups is also disadvantageous, because the terminal groups destabilize the framework (Hao et al. 2010; Tang and Landskron 2010). Therefore, it is necessary to develop a method to synthesize meso-materials with a highly symmetrical amino-group distribution.

The AFMS materials with well ordered structure were synthesized by self-assembly of anionic surfactants and inorganic precursors, by which amino groups could be distributed uniformly due to the introduction of aminosilane or quaternized aminosilane as CSDA (Che et al. 2003; Zheng et al. 2008). In our previous work, the AFMS spheres with centrosymmetric radial mesopores were synthesized using the anionic surfactant Sar-Na as template and APTMS as CSDA but the amino loadings in the synthesized AFMS samples were relatively low (Hao et al. 2010). Later on we used an orthogonal experiment optimization to synthesize the amino-functionalized silica spheres with centrosymmetric radial mesopores and high amino loading, which were used as adsorbent for the removal of Cu^{2+} and Pb^{2+} from aqueous solutions, showing some excellent removal properties (Hao et al. 2012). Predicatively, a high amino loading in the AFMS would improve CO_2 adsorption properties in terms of adsorption capacity and selectivity and the available centrosymmetric radial mesopores connected to each other would lead to better CO_2 diffusion properties.

In the present study, the synthesis of the amino-functionalized silica spheres with centrosymmetric radial mesopores and high amino loading was optimized and the synthesized AFMS adsorbent was used for selective CO_2 adsorption. Because water vapor is always present during the separation or purification of CO_2 from natural gas, for instance, the effects of water vapor on CO_2 adsorption on the synthesized AFMS adsorbent were investigated in detail. Finally, the applicability of the synthesized AFMS adsorbent was anticipated for CO_2 adsorption and separation.

2 Experimental

2.1 Synthesis and characterization of AFMS adsorbent

The synthesis of AFMS adsorbent was optimized by an orthogonal experiment design (Hao et al. 2012). Under the optimized recipe and synthesis conditions, 2.347 g of Sar-Na (from Merck) was completely dissolved in 70 ml of deionized water under stirring at room temperature. Afterward, 25 ml of 0.1 M HCl solution (prepared from 37 % fuming hydrochloric acid from Sinopharm Chemical Reagent Co., Ltd., Shanghai) was added into the prepared Sar-Na solution under vigorous stirring for 1 h and then a mixture of 4.0 ml TEOS (from Acros) and 0.60 ml of APTMS (from Aldrich) was added into the above prepared solution under vigorous stirring for 10 min. The resulting mixture was aged at room temperature for 2 h and the synthesis was then hydrothermally carried out without agitation in a closed 100 ml reaction kettle placed in an oven at 80 °C for 24 h. The product was filtered and the solid was washed with deionized water. The washed solid was then dried for 10 h at 80 °C prior to a further analysis or use. The surfactant in the dried sample was removed by an extraction method (Zheng et al. 2008). 1.0 g of the dried solid was dispersed in a mixture solution of 80 ml of ethanol and 20 ml of ethanol amine at room temperature under agitation and then the mixture was refluxed at 90 °C for 12 h. The solid was recovered by filtration, washed with ethanol, and dried. The above extraction procedure was repeated twice.

The synthesized samples were characterized by FT-IR, SEM, TEM, N_2 adsorption-desorption, and elemental analysis techniques. The detailed description of the instruments and experimental procedures is reported elsewhere (Hao et al. 2010).

2.2 Adsorption experiment

The adsorption isotherms of CO_2, N_2, and CH_4 on the AFMS adsorbent were measured with Micromeritics ASAP 2020. The sample cell was loaded with ca. 250 mg of the adsorbent. After the adsorbent was outgassed in vacuum at 120 °C for 12 h in order to remove any adsorbed impurities, the adsorption run was carried out using highly pure CO_2 (99.999 %), N_2 (99.99 %), and CH_4 (99.99 %) in a pressure range from 0.01 to 101 kPa.

The temperature-programmed desorption (TPD) of CO_2 performed on a Micromeritics AutoChem II analyzer was used to measure the stability of the adsorbent and a house-made TPD-MS analyzer (Balzer Ominstar 200) was used to investigate the effects of water vapor on the adsorption of CO_2. These experimental procedures are reported elsewhere (Hao et al. 2011).

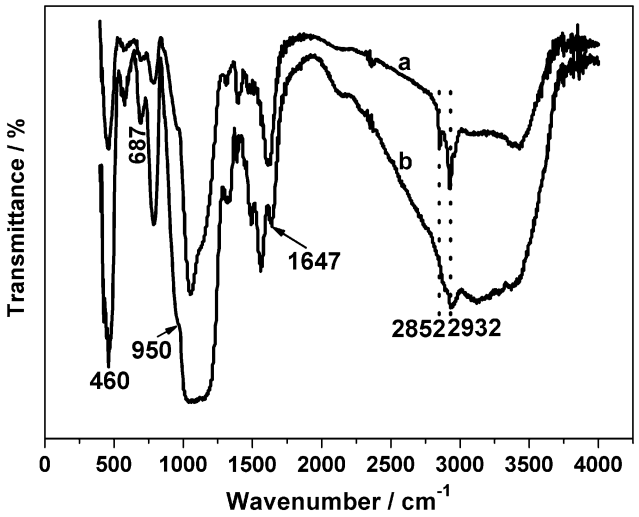

Fig. 1 FT-IR spectra of the as-synthesized sample (**a**) and the extracted sample (**b**)

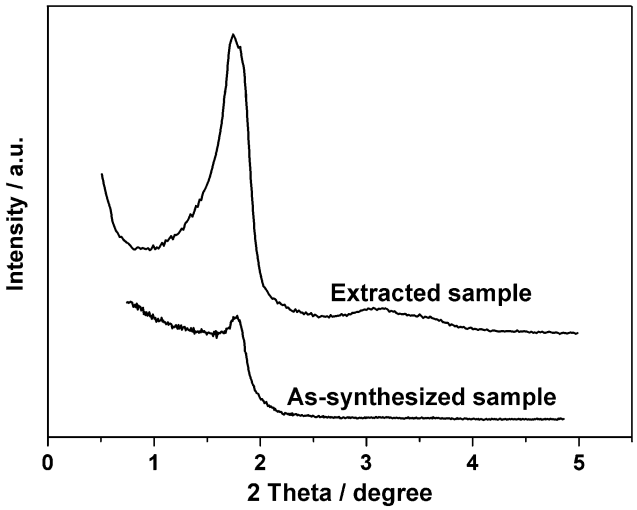

Fig. 2 XRD patterns of the as-synthesized and extracted samples

3 Results and discussion

3.1 Textural and physicochemical properties

The FT-IR spectra of the as-synthesized and extracted samples are shown in Fig. 1. According to Zheng et al. (2008), the amount of the surfactant and of the CSDA in the sample can be reflected from the intensity of bands around 2852 and 2932 cm^{-1}, which can be associated with the symmetrical and asymmetrical stretching vibrations of the methylene groups of the surfactant and the CSDA, respectively. From Fig. 1, it is also found that the intensity of typical methylene bands in the extracted sample is dramatically lower than that of the as-synthesized one and the band of 2852 cm^{-1} in the extracted sample disappears, while the remaining weak peak at 2932 cm^{-1} could be associated with the methylene groups in the CSDA, which reveals that the surfactant has been removed from the as-synthesized sample. For the extracted sample (Fig. 1b), the broad absorption band in the region of 3765–3055 cm^{-1} can be attributed to the stretching of the framework Si–OH group and physically adsorbed water molecules. Apart from the region of 3765–3055 cm^{-1}, the presence of silanol groups is also confirmed by the weak peak at around 950 cm^{-1}, associated with non-condensed Si–OH groups. The vibrations of Si–O–Si can be seen at around 1095 cm^{-1} (asymmetric stretching) and 460 cm^{-1} (bending) (Umamaheswari et al. 2002). The presence of –N–H bending vibration around 687 and 1650 cm^{-1} and $–NH_2$ scissor vibration around 1647 cm^{-1} confirms the existence of amino groups (Hao et al. 2011; Heidaria et al. 2009). The presence of aminopropyl groups in the AFMS is further corroborated by a broad band at 2700–3500 cm^{-1}, ascribed to the –N–H stretching around 3346 cm^{-1} for free amine and around 3305 cm^{-1} for terminal amino groups, respectively (White and Tripp 2000), while the stretching always overlaps with the broad absorption band of the silanol group and physically adsorbed water molecules.

Figure 2 presents the XRD patterns of the as-synthesized and extracted samples. There are distinguishable diffraction peaks around $2\theta = 1.75°$ for these two samples. However, the peak intensity of the extracted sample is much higher than that of the as-synthesized one. Moreover, the broad peaks in the region of $2\theta = 2.7–4.0°$ can be detected on the XRD curve of the extracted sample, probably resulted from the removal of the surfactant.

Figure 3 depicts the adsorption-desorption isotherms of N_2 on the as-synthesized and extracted samples at −196 °C and their corresponding pore-size distribution plot derived by the density functional theory (DFT) model. From Fig. 3a, it can be seen that the adsorption isotherm of N_2 on the extracted sample displays a type-IV isotherm with H1 hysteresis and has a steep increase in the adsorbed amount in a relative pressure range of 0.35–0.56, implying that the extracted sample possesses a well-ordered mesostructure. In comparison, the adsorbed amounts of N_2 on the as-synthesized sample in the whole relative pressure range are much lower, and the initial capillary condensation step shifts to a lower relative pressure of 0.15. For the extracted sample, the estimated BET surface area is 553 m^2/g and the total pore volume is 0.59 cm^3/g while the estimated BET surface area is 323 m^2/g and the total pore volume is 0.14 cm^3/g for the as-synthesized sample. As shown in Fig. 3b, the pore size distribution of the extracted sample is centered at about 3.7 nm, whereas it is at about 2.3 nm for the as-synthesized sample. These results imply that a large amount of the surfactant Sar-Na was removed after extraction by ethanol and amine ethanol, in good agreement with the results of FT-IR.

The SEM and TEM images of the extracted sample are shown in Fig. 4. The SEM image displays that the obtained

sample is composed of silica spheres and all the spheres are segregated. The TEM image shows that the centrosymmetric radial mesopores emanate from the spherical center to the exterior surface and uniform projections with the same pore arrangement patterns appear in all the spheres, indicating that the spherical morphology is indeed produced in all the particles and the pores are distributed in a spherically symmetric mode.

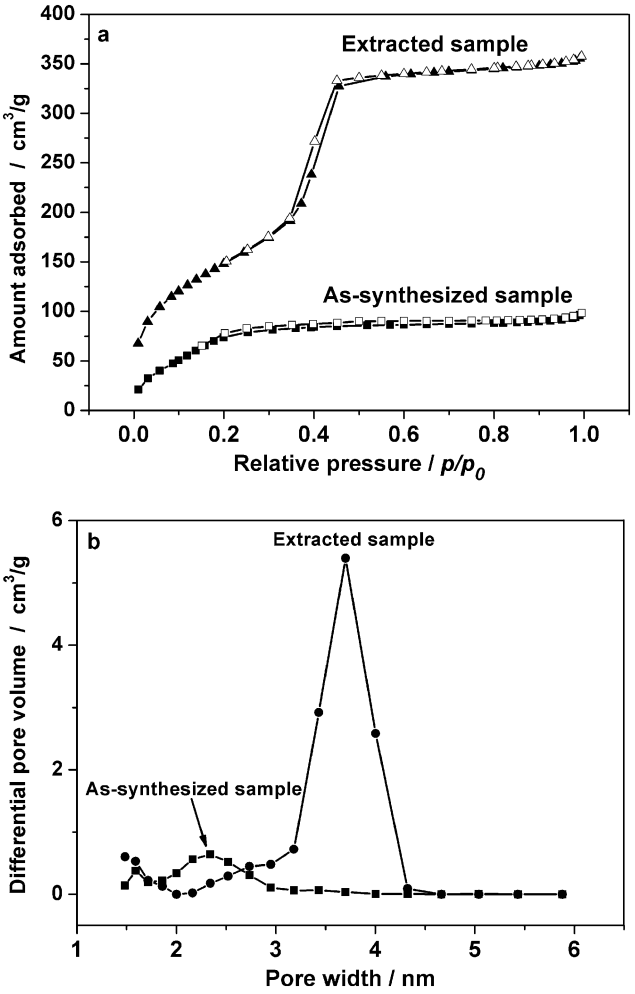

Fig. 3 Adsorption-desorption isotherms of N_2 on the as-synthesized and extracted samples at −196 °C (**a**) and the corresponding DFT pore size distribution plot from the adsorption branch (**b**)

Compared to the previously synthesized sample (Hao et al. 2010), the current AFMS sample has a larger BET surface area, a higher pore volume, and a higher amino loading. It has been reported that the long-range ordering of the mesostructure decreases with increasing the APTMS concentration in the initial synthesis solution (Chong and Zhao 2003; Hao et al. 2011; Wang et al. 2005). In the current synthesis, the used dosage of APTMS was about 2.6 times as large as that used in our previous synthesis (Hao et al. 2010), leading to a higher amino loading in the resulting AMFS sample. Although the addition of APTMS into the initial synthesis solution can adversely affect the mesostructure, the ordered mesostructure of the AFMS can be reserved by optimizing the pH in the initial synthesis solution. It is clear that Sar–Na is protonated to form N-lauroylsarcosine acid (Sar–H) after 0.1 M HCl solution added. The amino groups in APTMS, therefore, interact with Sar–H via a neutralization mechanism after the mixture of APTMS and TEOS is added into the solution containing Sar–H, in which the interaction between amino groups and Sar–H becomes stronger and yet this interaction is selective, leading to a high loading and a highly symmetrical distribution of amino groups in the resulting AFMS. Furthermore, it is beneficent for the hydrolysis and condensation of silicates such as TEOS, APTMS, and their oligomers under a reasonably acidic system (Hao et al. 2012).

3.2 Adsorption properties

The adsorption isotherms of CO_2, N_2, and CH_4 on the extracted sample at 25 °C are plotted in Fig. 5. It is clear that the adsorbed amount of CO_2 on the extracted sample arrives at 2.36 mmol/g at 101 kPa, much higher than 1.84 mmol/g

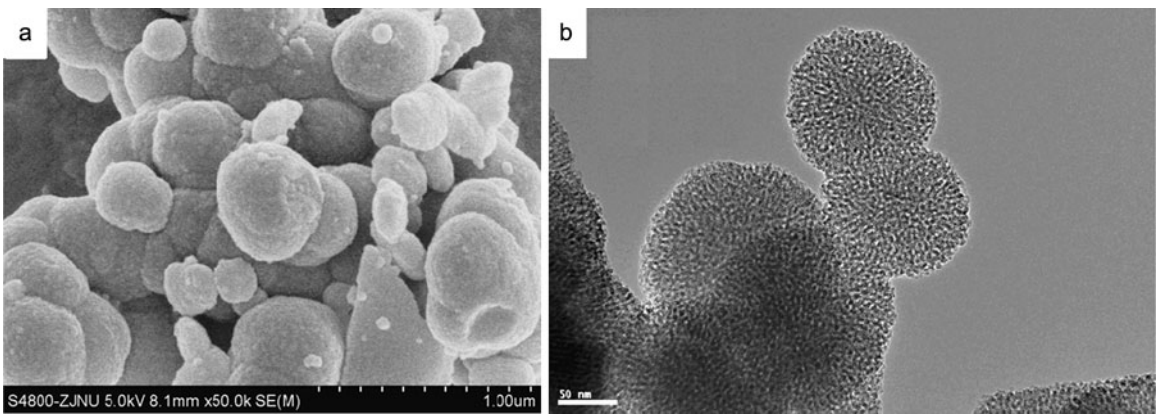

Fig. 4 SEM (**a**) and TEM (**b**) images of the AFMS adsorbent

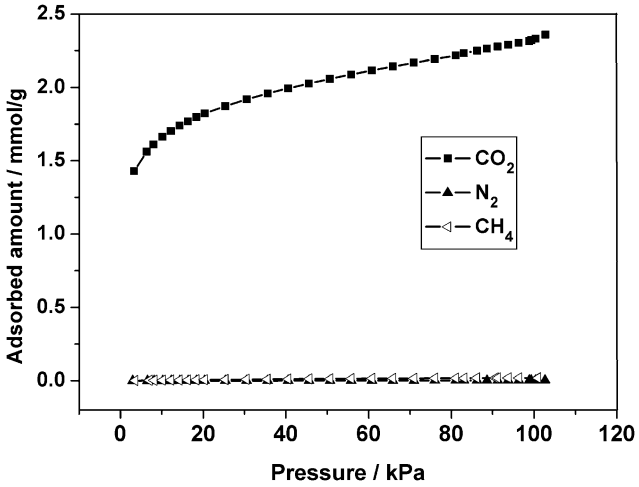

Fig. 5 Adsorption isotherms of CO_2, N_2, and CH_4 on the AFMS adsorbent at 25 °C

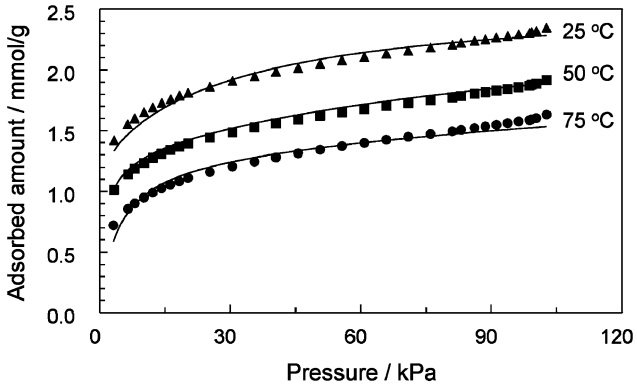

Fig. 6 Adsorption isotherms of CO_2 on the AFMS adsorbent at 25 °C, 50 °C, and 75 °C. Lines are the dual-site Langmuir model correlation

on the amine-grafted SBA-15 (Tang and Landskron 2010), 0.40 mmol g^{-1} on the PEI surface-modified MCM-48 (Kim et al. 2005), and 1.25 mmol g^{-1} on the amino-functionalized mesoporous silica (Kim et al. 2008) under the same conditions. The reason for the higher adsorbed capacity of CO_2 would be related to the amino groups loaded in the adsorbent for the formation of ammonium carbamates and/or carbonates. Generally, a higher amino loading will lead to a higher CO_2 adsorption capacity. The N content in the AFMS adsorbent is 6.37 mmol/g, determined by the elemental analysis, much higher than those reported in the literature (Hao et al. 2010; Tang and Landskron 2010; Zelenak et al. 2008), resulting in a favorable CO_2 adsorption. Furthermore, more silanol groups can be reserved on the surface of the AFMS adsorbent where the template was removed by the extraction method, which would be helpful for improving CO_2 adsorption capacity (Yue et al. 2008). In order to determine the ideal selectivity for CO_2 over N_2 and CH_4, the adsorption isotherms of N_2 and CH_4 were also measured, as shown in Fig. 5. Compared with the isotherm of CO_2, the adsorption of N_2 and CH_4 is negligible under the investigated conditions, although the adsorbed amounts of both N_2 and CH_4 increase with increasing pressure. The ideal adsorption selectivity for CO_2 over N_2 is more than 2,000 at 25 °C and 101 kPa, much higher than 131 on the amine-grafted SBA-15 (Wang and Yang 2011), 14 on the nanostructured templated carbon (Wang and Yang 2012), 308 on the tri-amino surface-modified pore-expanded MCM-41 (Belmabkhout and Sayari 2009), and 18 on zeolite-13X (Siriwardane et al. 2001) under the same conditions. The adsorption selectivity for CO_2 over CH_4 arrives at 125 at 25 °C and 101 kPa, much higher than 5.7 on the ordered mesoporous silica molecular sieve-SBA-15 (Liu et al. 2005) and 16.1 on the amine-grafted MCM-48 (Huang and Yang 2003) under the same conditions.

The adsorption isotherms of CO_2 on the AFMS at temperatures of 25, 50, and 75 °C are plotted in Fig. 6. Various isotherm models, such as the Langmuir, dual-site Langmuir, Unilan, Tóth, and Sips models have been considered, but the dual-site Langmuir model describes the present case much better over the full range.

$$q = q_{\mathrm{A}}^{\mathrm{sat}} \frac{K_{\mathrm{A}} p}{1 + K_{\mathrm{A}} p} + q_{\mathrm{B}}^{\mathrm{sat}} \frac{K_{\mathrm{B}} p}{1 + K_{\mathrm{B}} p} \tag{1}$$

where q is the adsorbed amount, p is the equilibrium pressure, $q_{\mathrm{A}}^{\mathrm{sat}}$ and K_{A} are the saturation capacity and the affinity parameter (equilibrium constant) on the first set of sites, respectively, and $q_{\mathrm{B}}^{\mathrm{sat}}$ and K_{B} are the analogous parameters on the second set of sites. By convention, we assume that the first set of sites has the larger affinity parameter, i.e., $K_{\mathrm{A}} > K_{\mathrm{B}}$. In the dual-site Langmuir model, the parameters K_{A} and K_{B} are temperature dependent and take the usual van't Hoff relation that can be written as:

$$K_i = K_{i0} \exp\left(\frac{-\Delta H_i^{\mathrm{ads}}}{R_g T}\right), \quad i = \mathrm{A}, \mathrm{B} \tag{2}$$

where K_{i0} are the equilibrium constants at infinite temperature, $\Delta H_i^{\mathrm{ads}}$ are the adsorption enthalpy changes, R_g is the universal gas constant, and T is the temperature studied. The isotherm data can be fairly described by the combined fitting (Peng et al. 2010; Zhu et al. 2001), i.e., Eqs. (1) and (2), as shown in Fig. 6 by the drawn lines. The estimated parameter values are listed in Table 1. Under dried conditions, i.e., in the absence of water vapor, two moles of amino groups are required to react with one mole of CO_2 to form one mole of carbamates (Hao et al. 2011), indicating that a total adsorption saturation capacity of 2.6 mmol/g corresponds to an amount of the amino groups of 5.2 mmol/g that is much lower than the measured value of the amino groups loaded in the adsorbent (about 6.4 mmol/g), based on CO_2 reacting with the amino groups to form carbamates for CO_2 adsorption. This is probably ascribed to the facts that some of the

Table 1 Estimated parameter values and 95 % confidence limits for the combined fitting of the isotherm data of CO_2 on the AFMS by the dual-site Langmuir model

q_A^{sat}	q_B^{sat}	$K_{A0} \times 10^8$	$K_{B0} \times 10^9$	$-\Delta H_A^{ads}$	$-\Delta H_B^{ads}$
mmol/g		kPa^{-1}		kJ/mol	
1.29 ± 0.03	1.30 ± 0.04	1.10 ± 1.91	1.58 ± 0.86	49.02 ± 5.07	41.67 ± 1.40

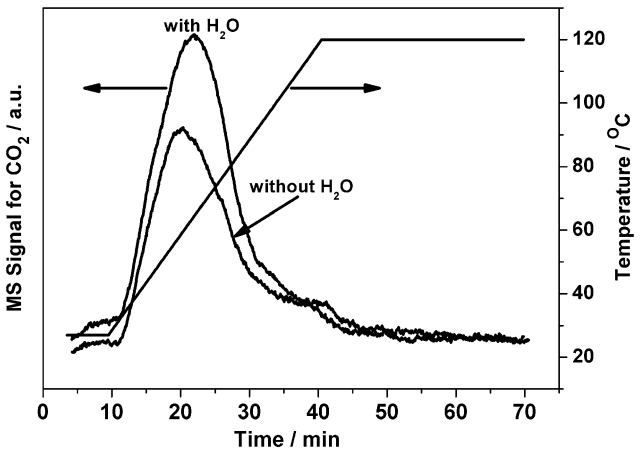

Fig. 7 Effects of water vapor on the adsorption of CO_2 on the AFMS adsorbent

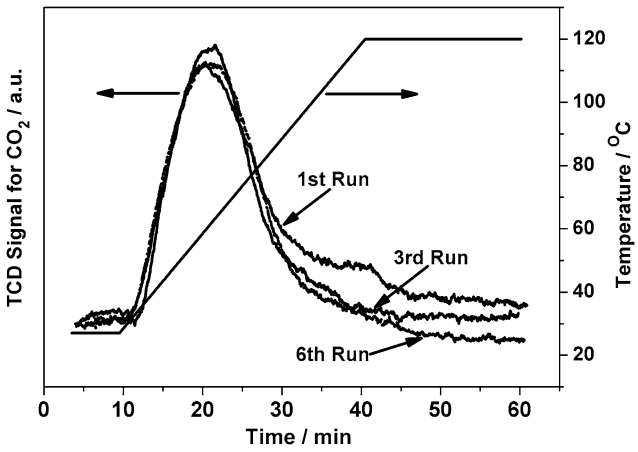

Fig. 8 Multi-cycle TPD profiles of CO_2 on the AFMS adsorbent

functional groups might be embedded in the silica network or the amino groups loaded on the surface of the small pores could not adsorb CO_2.

Based on the measured isotherms of CO_2 at the three different temperatures, the isosteric heat (Q^{st}) of adsorption as a function of loading was calculated, and the results show that Q^{st} slightly decreases with increasing CO_2 loading from 0 to 1.3 mmol/kg. The isosteric heat of adsorption at zero coverage (Q_0^{st}) in the current case is about 49 kJ/mol, much higher than 25 kJ/mol on the all-silica zeolite silicalite-1 (Zhu et al. 2006), slightly higher than 47 kJ/mol on the aminopropyl-functionalized ITQ-6/AP (Zukal et al. 2009) and 45 kJ/mol on Na-FER with a Si/Al molar ratio of 26.6 (Pulido et al. 2009), lower than 52 kJ/mol on Na-FER with a Si/Al molar ratio of 8.6 (Pulido et al. 2009) and 65 kJ/mol on the aminopropyl-functionalized SBA-15/AP2 (Zukal et al. 2009). These results clearly indicate that there are the specific interactions between CO_2 and the amino groups involved in the adsorption on the AFMS adsorbent. On the other hand, the moderate isosteric heat of adsorption implies the medium interactions between CO_2 and adsorbent, which could be beneficial to the regeneration of the AFMS adsorbent.

Water vapor often plays an important role of proton transfer agent in the reaction of CO_2 and amino groups (Hao et al. 2011). Figure 7 shows the desorption patterns after CO_2 adsorption under dry or humid conditions to elucidate the effects of water vapor on the adsorption of CO_2 on the AFMS adsorbent. Clearly, after the adsorption of CO_2 saturated with water vapor at 25 °C, the desorption-peak area is larger, compared to that after CO_2 adsorption under the dry conditions. These results demonstrate that the presence of water vapor can enhance the adsorbed amount of CO_2, which can be explained by the basis of the mechanism of reactions between CO_2 and amino groups as follows: two moles of amino groups are required to react with one mole of CO_2 to form one mole of carbamates in the absence of water vapor, whereas partial carbamates will be changed into bicarbonate in the presence of water and one mole of amino groups react with one mole of CO_2 to form one mole of bicarbonates in the presence of moisture (Hao et al. 2011; Huang and Yang 2003).

In specific interactions involved adsorption for CO_2 separation, temperature swing adsorption (TSA) is a common process, in which rising operating temperature can enhance the desorption rate of the adsorbed CO_2. Therefore, the thermal stability of CO_2 adsorbents is crucial in practical applications. In order to check the thermal stability of the AFMS adsorbent, the multi-cycles of CO_2 adsorption at 25 °C and temperature-programmed desorption (TPD) were performed. Figure 8 represents six-cycle TPD profiles of CO_2 on the AFMS adsorbent. It can be found that the third- and sixth-run TPD profiles are almost identical to the first-run one, implying that the adsorbent is thermally stable and recyclable.

The developed AFMS adsorbent shows some excellent properties for CO_2 adsorption, including high adsorption capacity and high reusability, displaying a good prospect for practical applications in the selective adsorption of CO_2.

4 Conclusions

The AFMS spheres with centrosymmetric radial mesopores and high amino-group loading were optimally synthesized. The AFMS adsorbent has a high adsorption capacity and a high selectivity for CO_2 over N_2 and CH_4 due to the intensive interactions between amino groups and CO_2. The presence of water vapor can enhance the adsorbed amount of CO_2 because of the partial formation of bicarbonate in the presence of moisture. The adsorption-regeneration cycle experiments confirm that the developed adsorbent is thermally stable and recyclable. Based on these excellent properties, the AFMS adsorbent displays a good prospect for practical applications in the selective adsorption of CO_2.

Acknowledgements The financial support by the National Natural Science Foundation of China (20971109 and 21036006), the Program for Changjiang Scholars and Innovative Research Team in Chinese Universities (IRT0980), and the Zhejiang Provincial Natural Science Foundation of China (Y4110289, R4080084) is gratefully acknowledged.

References

Belmabkhout, Y., Sayari, A.: Effect of pore expansion and amine functionalization of mesoporous silica on CO_2 adsorption over a wide range of conditions. Adsorption **15**, 318–328 (2009)

Belmabkhout, Y., Serna-Guerrero, R., Sayari, A.: Adsorption of CO_2-containing gas mixtures over amine-bearing pore-expanded MCM-41 silica: application for gas purification. Ind. Eng. Chem. Res. **49**, 359–365 (2010)

Bhide, B.D., Voskericyan, A., Stern, S.A.: Hybrid processes for the removal of acid gases from natural gas. J. Membr. Sci. **140**, 27–49 (1998)

Che, S., Garcia-Bennett, A.E., Yokoi, T., Sakamoto, K., Kunieda, H., Terasaki, O., Tatsumi, T.: A novel anionic surfactant templating route for synthesizing mesoporous silica with unique structure. Nat. Mater. **2**, 801–806 (2003)

Chong, A.S.M., Zhao, X.S.: Functionalization of SBA-15 with APTES and characterization of functionalized materials. J. Phys. Chem. B **107**, 12650–12657 (2003)

Da'na, E., Sayari, A.: Adsorption of copper on amine-functionalized SBA-15 prepared by co-condensation: equilibrium properties. Chem. Eng. J. **166**, 445–453 (2011)

Du, X., He, J.: Hierarchically mesoporous silica nanoparticles: extraction, amino-functionalization, and their multipurpose potentials. Langmuir **27**, 2972–2979 (2012)

Hao, S.Y., Xiao, Q., Yang, H., Zhong, Y.J., Pepe, F., Zhu, W.D.: Synthesis and CO_2 adsorption property of amino-functionalized silica nanospheres with centrosymmetric radial mesopores. Microporous Mesoporous Mater. **132**, 552–558 (2010)

Hao, S.Y., Chang, H., Xiao, Q., Zhong, Y.J., Zhu, W.D.: One-pot synthesis and CO_2 adsorption properties of ordered mesoporous SBA-15 materials functionalized with APTMS. J. Phys. Chem. C **115**, 12873–12882 (2011)

Hao, S.Y., Zhong, Y.J., Pepe, F., Zhu, W.D.: Adsorption of Pb^{2+} and Cu^{2+} on anionic surfactant-templated amino-functionalized mesoporous silicas. Chem. Eng. J. **189–190**, 160–167 (2012)

Heidaria, A., Younesia, H., Mehraban, Z.: Removal of Ni(II), Cd(II), and Pb(II) from a ternary aqueous solution by amino functionalized mesoporous and nano mesoporous silica. Chem. Eng. J. **153**, 70–79 (2009)

Himeno, S., Komatsu, T., Fujita, S.: High-pressure adsorption equilibria of methane and carbon dioxide on several activated carbons. J. Chem. Eng. Data **50**, 369–376 (2005)

Huang, H.Y., Yang, R.T.: Amine-grafted MCM-48 and silica xerogel as superior sorbents for acidic gas removal from natural gas. Ind. Eng. Chem. Res. **42**, 2427–2433 (2003)

Kim, S., Ida, J., Guliants, V.V., Lin, J.Y.S.: Tailoring pore properties of MCM-48 silica for selective adsorption of CO_2. J. Phys. Chem. B **109**, 6287–6293 (2005)

Kim, S.N., Son, W.J., Choi, J.S., Ahn, W.S.: CO_2 adsorption using amine-functionalized mesoporous silica prepared via anionic surfactant-mediated synthesis. Microporous Mesoporous Mater. **115**, 497–503 (2008)

Lawal, O., Bello, A., Idem, R.: The role of methyl diethanolamine (MDEA) in preventing the oxidative degradation of CO_2 loaded and concentrated aqueous monoethanolamine (MEA)-MDEA blends during CO_2 absorption from flue gases. Ind. Eng. Chem. Res. **44**, 1874–1896 (2005)

Liu, X., Li, J., Zhou, L., Huang, D., Zhou, Y.: Adsorption of CO_2, CH_4 and N_2 on ordered mesoporous silica molecular sieve. Chem. Phys. Lett. **415**, 198–201 (2005)

Na, B.K., Lee, H., Koo, K.K., Song, H.K.: Effect of rinse and recycle methods on the pressure swing adsorption process to recover CO_2 from power plant flue gas using activated carbon. Ind. Eng. Chem. Res. **41**, 5498–5503 (2002)

Peng, Y., Zhang, F.M., Zheng, X., Wang, H.Y., Xu, C.H., Xiao, Q., Zhong, Y.J., Zhu, W.D.: Comparison study on the adsorption of CFC-115 and HFC-125 on activated carbon and silicalite-1. Ind. Eng. Chem. Res. **49**, 10009–10015 (2010)

Pulido, A., Nachtigall, P., Zukal, A., Domínguez, I., Čejka, J.: Adsorption of CO_2 on sodium-exchanged ferrierites: the bridged CO_2 complexes formed between two extraframework cations. J. Phys. Chem. C **113**, 2928–2935 (2009)

Richer, R., Mercier, L.: Direct synthesis of functionalized mesoporous silica by non-ionic alkylpolyethyleneoxide surfactant assembly. Chem. Commun. **16**, 1775–1777 (1998)

Sandru, M., Kim, T.J., Hagg, M.B.: High molecular fixed-site-carrier PVAm membrane for CO_2 capture. Desalination **240**, 298–300 (2009)

Siriwardane, R.V., Shen, M.S., Fisher, E.P., Poston, J.A.: Adsorption of CO_2 on molecular sieves and activated carbon. Energy Fuels **15**, 279–284 (2001)

Song, C.: Global challenges and strategies for control, conversion and utilization of CO_2 for sustainable development involving energy, catalysis, adsorption and chemical processing. Catal. Today **115**, 2–32 (2006)

Tang, Y., Landskron, K.: CO_2-sorption properties of organosilicas with bridging amine functionalities inside the framework. J. Phys. Chem. C **114**, 2494–2498 (2010)

Umamaheswari, V., Palanichamy, M., Murugesan, V.: Isopropylation of m-cresol over mesoporous Al-MCM-41 molecular sieves. J. Catal. **210**, 367–374 (2002)

Veawab, A., Tontiwachwuthikul, P., Chakma, A.: Corrosion behavior of carbon steel in the CO_2 absorption process using aqueous amine solutions. Ind. Eng. Chem. Res. **38**, 3917–3924 (1999)

Veawab, A., Tontiwachwuthikul, P., Chakma, A.: Investigation of low-toxic organic corrosion inhibitors for CO_2 separation process using aqueous MEA solvent. Ind. Eng. Chem. Res. **40**, 477–4777 (2001)

Wang, L., Yang, R.T.: Increasing selective CO_2 adsorption on amine-grafted SBA-15 by increasing silanol density. J. Phys. Chem. C **115**, 21264–21272 (2011)

Wang, L., Yang, R.T.: Significantly increased CO_2 adsorption performance of nanostructured templated carbon by tuning surface area and nitrogen doping. J. Phys. Chem. C **116**, 1099–1106 (2012)

Wang, X.G., Lin, K.S.K., Chan, J.C.C., Cheng, S.: Direct synthesis and catalytic applications of ordered large pore aminopropyl-functionalized SBA-15 mesoporous materials. J. Phys. Chem. B **109**, 1763–1769 (2005)

White, L.D., Tripp, C.P.: Reaction of (3-Aminopropyl)dimethylethoxysilane with amine catalysts on silica surfaces. J. Colloid Interface Sci. **232**, 400–407 (2000)

Yue, M.B., Sun, L.B., Cao, Y., Wang, Z.J., Wang, Y., Yu, Q., Zhu, J.H.: Promoting the CO_2 adsorption in the amine-containing SBA-15 by hydroxyl group. Microporous Mesoporous Mater. **114**, 74–81 (2008)

Zelenak, V., Halamova, D., Gaberova, L., Bloch, E., Llewellyn, P.: Amine-modified SBA-12 mesoporous silica for carbon dioxide capture: effect of amine basicity on sorption properties. Microporous Mesoporous Mater. **116**, 358–364 (2008)

Zheng, H., Gao, C., Che, S.: Amino and quaternary ammonium group functionalized mesoporous silica: an efficient ion-exchange method to remove anionic surfactant from AMS. Microporous Mesoporous Mater. **116**, 299–307 (2008)

Zhu, W., Kapteijn, F., Linden, B., Moulijn, J.A.: Equilibrium adsorption of linear and branched C_6 alkanes on silicalite-1 studied by the tapered element oscillating microbalance. Phys. Chem. Chem. Phys. **3**, 1755–1761 (2001)

Zhu, W.D., Hrabanek, P., Gora, L., Kapteijn, F., Moulijn, J.A.: Role of adsorption in the permeation of CH_4 and CO_2 through a silicalite-1 membrane. Ind. Eng. Chem. Res. **45**, 767–776 (2006)

Zukal, A., Dominguez, I., Mayerová, J., Čejka, J.: Functionalization of delaminated zeolite ITQ-6 for the adsorption of carbon dioxide. Langmuir **25**, 10314–10321 (2009)